Z. Phys. D – Atoms, Molecules and Clusters 5, 293–298 (1987)

Atoms, Molecules and Clusters
Zeitschrift für Physik D

Phase Space Approach to Above Threshold Ionization

J. Mostowski*
Max-Planck-Institut für Quantenoptik, Garching, Federal Republic of Germany

K. Zyczkowski
Institute of Physics, Jagiellonian University, Cracow, Poland

Received October 27, 1986

Phase space averaging method of classical mechanics is applied to the study of strong field ionization of atoms (ATI). The photoelectron spectra calculated by this simple method exhibit the main features of the spectra observed in numerous experiments. This approach provides a novel insight into the strong field processes and is the only one so far which can be applicable for intensities above 10^{14} W/cm^2.

PACS: 32.80.Rm; 42.50.Hz; 42.50.Tj

I. Introduction

Multiphoton ionization of atoms by strong laser pulses is a subject of considerable recent interest. It was established by many experiments [1] that for laser intensities above a certain threshold the spectrum of the outgoing photoelectrons consists of many peaks separated by photon energy. The relative sizes of the peaks depend on the laser intensity and in the region 10^{12}–10^{13} W/cm^2 they become inverted, i.e. peaks corresponding to higher electron energy become more populated than the lower energy peaks.

A number of theoretical ideas was formulated in order to explain the shape of the photoelectron spectra and other features of ATI. Although they are based on different physical principles it is probable that they are complementary rather than conflicting.

Some of the theoretical papers are based on the idea that the ponderomotive force determines the shape of the photoelectron spectrum [2], although some experiments claim a total absence of the ponderomotive effect [3]. Another interesting approach is based on the observation that the photoelectron are produced in a form of a charged cloud and hence the electrostatic interaction between the charges should be taken into account [4]. This Coulomb interaction should be responsible for decreasing the size of the low energy peaks in the photoelectron spectrum. It should be noted, however, that some experiments [5] are done at such a low density that the space charge effects are believed to be absent.

A different kind of approach points out the importance of the continuum-continuum transitions and their saturation [6]. This approach, although quite sucessful, is restricted to laser field strengths below a certain threshold [7], typically of the order of 10^{14} W/cm^2.

In the present paper we develop yet another model of ATI which we call the phase space averaging method. This method is based on the assumption that the electron can be treated in the framework of classical, rather than quantum mechanics. In a potential with a parabolic minimum the initial (i.e. ground) state of the electron can be adequately approximated by a harmonic oscillator ground state. It is well known that in this case the classical solution is a good approximation to the quantum problem. The classical approximation becomes even better when the electron becomes excited.

This is not the first paper where the phase space averaging method of classical mechanics is used to describe the process of ionization. The method was sucessfully applied to the problems of multiphoton transitions in strong fields for the case of Rydberg atoms in a strong rf field [8] and surface electrons in a semiconductor layer structure [9]. The applica-

* Alexander von Humboldt scholar 1986/87. Permanent address: Institute of Physics, Polish Academy of Sciences, Aleja Lotnikow 32/46, PL-02-668 Warszawa, Poland

tion of this method was in a sense natural, because the quantum systems under consideration there were in highly excited states. Here we would like to extend this method to a less obvious case of systems initially in their ground states. We will discuss the validity of this approach in the last Section.

In this paper we consider a one dimensional model of an atom. The binding interaction is taken to be Rosen-Morse potential. The interaction with the laser field will be approximated in this paper by a series of "kicks" or pulses. Although this approximation is not an essential one it simplifies to a great extend the numerical calculations. Such approximation was used also by Blümmel and Meir [10] in their recent model of ionization. Also such a pulsed interaction was often used in the study of chaotic, classical or quantum, systems [11]. The pulsed interaction allows to replace the differential equations of motion (Newton's equations in the classical case or Schrödinger equation in the quantum case) by a discrete map, much easier to study numerically. The price for such simplification is the introduction of "higher frequency photons", which, fortunately, play only a marginal role [12].

The paper is organized as follows. In Sect. II we define our model. In Sect. III we discuss the results of the phase averaging method applied to the study of strong field ionization and draw conclusions regarding the photoelectron spectrum in ATI. In the Appendix some details of the calculations are presented.

II. The Model

Our model consists of a single electron with mass m subject to a potential $U(x)$. The position and momentum of the electron are denoted by x and p respectively. We treat one dimensional motion only. Hamiltonian of the system, without the interaction with the external perturbation is given by:

$$H_0 = p^2/2m + U(x). \tag{1}$$

In our model calculations we will take the Rosen-Morse potential:

$$U(x) = U_0(\tanh^2(x/a) - 1) \tag{2}$$

to describe the atom. Here U_0 is the characteristic binding energy and a is the range of the iteraction.

We will treat the interaction with the external periodic field in the impulse approximation. This means that we will replace harmonic dependence of the electromagnetic field on time by a series of "kicks" or impulses. This means that for the interaction hamiltonian we will take:

$$H_I = K x \sum_{n=-\infty}^{\infty} (-1)^n \delta(t/2T - n). \tag{3}$$

Here K denotes the amplitude of the perturbation (corresponding to the electric field) and T is the period of the perturbation. We see from the formula above that the interaction consists of periodic pulses which act every half period with opposite signs. As can be easily seen each kick consists in adding (or substracting) the value K to the electron momentum. As mentioned in the Introduction such alternating impulses mimic the harmonic laser field.

In order to further elucidate the relation between the harmonic wave and the series of impulses given in formula (1) let us recall the Poisson formula:

$$\sum_{n=-\infty}^{\infty} \delta(x-n) = \sum_{m=-\infty}^{\infty} \exp(2\pi i m x). \tag{4}$$

If follows from the above formula that the perturbation in (1) containes, in addition to the fundamental frequency $\omega_L = 2\pi/T$ also higher harmonics $\pm(2n+1)\omega_L$ $(n=1,2\ldots)$. The role of the higher harmonics content on the photoelectron spectrum was considered in [12] where it was shown to be of little practical importance.

In order to model the quantum mechanical atom by classical quantities we took an ensamble of points in the phase space according to microcanonical distribution with a given energy E_0. This ensamble should describe a group of atoms in their ground states. Each point in the phase space defines the position and the momentum of electron at time $t=0$. This is the essence of the phase space averaging method – instead of wave function we take the classical microcanonical probability distribution. It should be noted that one may model the ground state by other classical probability distributions in the phase space, but we will not discuss this point further. We will, however, stress very strongly that we are not trying to develop any "classical" theory of atoms, what we are saying is that a class of atomic phenomena, namely the strong field ionization, can be described by classical models to a fair degree of accuracy.

The choice of the initial energy E_0 requires additional considerations. The microcanonical distribution should represent the ground state of the quantum-mechanical system. In the case of the Rosen-Morse potential the ground state energy is equal to:

$$E_0 = \hbar^2/4a^2 \left[\sqrt{(1 + 8U_0^2 a^2/\hbar^2)} - 1\right]^2. \tag{6}$$

This formula contains Planck constant $\hbar$ which comes from the solution of the Schrödinger equation. Know-

ing of the value of $\hbar$ from quantum mechanics we may correctly choose the value of E_0, which is, according to classical physics, completely arbitrary.

The classical microcanonical ensamble assumes that all points in the phase space are occupied with the same probability on a given energy surface. We have, therefore, to select points x_0, p_0 in the phase space according to such distribution. This is done most conveniently with the help of the Monte-Carlo method.

In order to proceed further let us introduce the natural units of length, time and mass. In the case of the Rosen-Morse potential the most natural choice of units is achieved by putting $m=1$, $a=1$, $U_0=1$. In other words we will measure the mass in units of electron mass, length in units of the potential range, and energy in units of binding potential U_0.

To study the time evolution of an element of the microcanonical ensamble, i.e. a single trajectory, a discrete map is derived from the equations of motion which follow from the hamiltonian (1), see [10–12]. The equations of motion can be solved separately for times between the pulses, this is just the free motion in the Rosen-Morse potential, and during each impulse. Details of the calculation are given in the Appendix. Figure 1 a–c shows the resulting trajectories (phase space points just after the impulses) for the same group of randomly selected 15 initial points and for three values of the impulse strength K. Each picture presents trajectories for up to 200 actions of the impulse perturbation. Some of the trajectories contain less points, if the trajectory left the range of the picture before 200 iterations were completed. Solid lines, which are shown for reference only, are separatrices, i.e. curves $E=0$.

It is seen from these figures that some trajectories form stable closed orbits in the phase space. The set of stable orbits form the region of regular motion. With the increase of the parameter K the area of regular motion decreases (Fig. 1 b) and finally (Fig. 1 c) only small stability islands remain. The rest of the phase space is occupied by chaotic trajectories. Some of these trajectories are bounded, confined to the potential well. Other orbits, however, gain energy fast and leave the range of the figure. This may be called classical ionization.

Inspection of Fig. 1 shows an interesting topological feature of the map – two curves can cross each other at one point of the phase space. This is because the points are plotted every half period of the perturbation.

Thus classical ionization should be associated with the existence of full scale chaos. Application of a perturbation which is strong enough causes disappearance of the KAM trajectories in the phase space

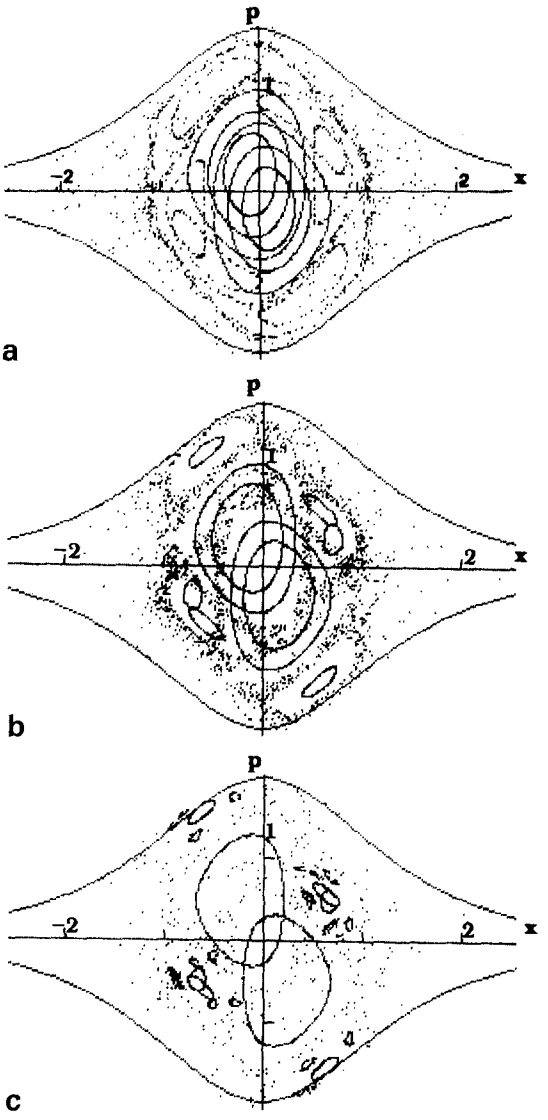

Fig. 1 a–c. Trajectories in the Rosen-Morse potential. 15 randomly chosen points in the phase space were iterated 200 times (100 periods). Solid lines denote $E=0$ curves. Period T is equal to 2, field strength K is equal to 0.3, 0.5 and 0.7 in **a**, **b** and **c** respectively

and connected stochasticity occurs. The trajectory diffuses for a while in the phase space until it gains enough energy to escape from the potential well. This diffusive mechanism of ionization was also pointed out in many papers dealing with the ionization of Rydberg atoms [8].

It should be stressed, however, that strictly speaking, trajectories which lead to ionization cannot be chaotic: Chaos is a long time property of a set of trajectories. Open trajectories are located within the range of the potential for a limited time only. For longer times they leave the region of the potential and become trajectories of free particles, subject to periodic impulses. These are definitely regular trajec-

tories. That is also why the diffusive absorption of energy from the impulses is bounded and does not take place for longer times. Chaotic, or erratic, behaviour of the trajectories is restricted to times during which the trajectory remains in the vicinity of the binding potential. Nevertheless we will use the term "diffusive absorption" or "diffusive ionization" being aware of its limitations.

III. Strong Field Ionization

In this Section we will discuss the process of ionization in strong fields with the help of the method described above.

When the perturbation is strong enough (large K) some trajectories can absorb enough energy to leave the region of atomic potential and thus ionize. In Fig. 2 we have presented ensamble of 100 trajectories with the initial energy equal to -0.9. As explained in Sect. II this is equivalent to assuming that $\hbar = 0.1414$ natural units. The map giving the motion was iterated 200 times (100 periods of the perturbing field) for two values of the field strength. The ionization channel of outgoing electrons is clearly seen. All electrons which aquired enough energy from the field move away from the atom. In the limit of large distance from the center the average momentum and energy of the electron become constant. This is because the atomic potential becomes constant at large distances.

In order to define classical ionization more precisely we introduced rather arbitrarily the atomic interaction range r_I, equal to 10 (or $10a$ in physical units). We say that ionization occurs if the energy of the outgoing photoelectron (averaged over the wave period) is positive and if the distance from the atom is larger than r_I. It is quite obvious that the exact value of r_I is not relevant (provided it is large enough) and does not influence the estimated values of the ionization probability.

Counting how many trajectories are open ones (classical ionization occurs) we may find the ionization probability. The results of such calculations are presented in Fig. 3. It displays the dependence of the ionization probability on the field strength K. Each curve corresponds to a different period T. For small values of the field the ionization does not take place. If K exceeds some critical value K_c, depending on T, the ionization probability growths quickly with the field up to saturation at 1. Contrary to the quantum case in the classical model ionization takes place only when the field is strong enough to break the KAM orbits and allow for diffusive energy uptake.

The ionization probability is in general an increasing function of the wave period T. This feature is easy to explain. For longer times of free evolution the outgoing electron with a positive energy gets further

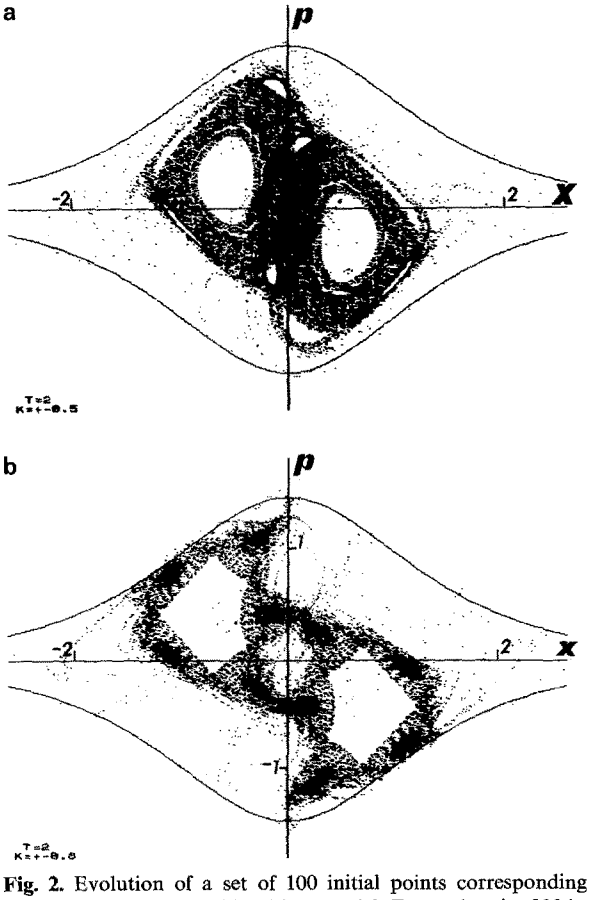

Fig. 2. Evolution of a set of 100 initial points corresponding to a microcanonical ensamble with $E = -0.9$. For each point 200 iterations were performed (or less if the point left the range of the picture). Period T is equal to 4, field strength $K = 0.5$ **a** and $K = 0.8$ **b**

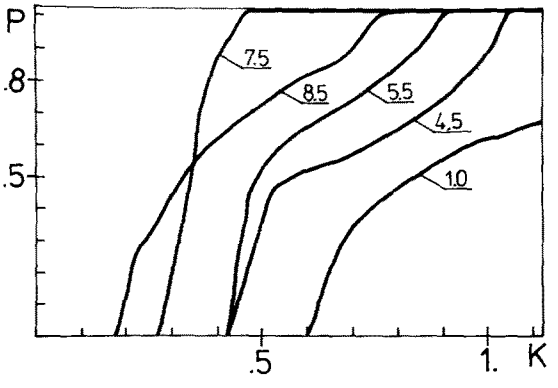

Fig. 3. Ionization probability as a function of the field strength for various half periods T. 800 initial points were used to represent the microcanonical ensamble with $E = -0.9$

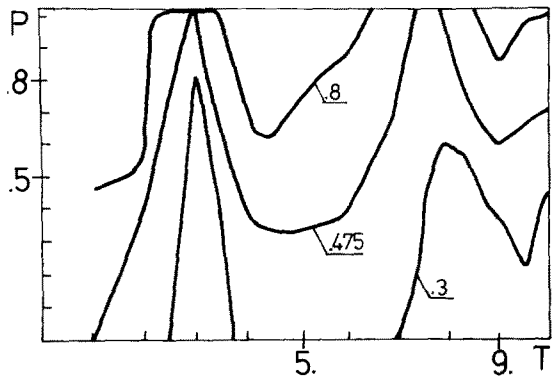

Fig. 4. Ionization probability as a function of field half period for various field strengths.

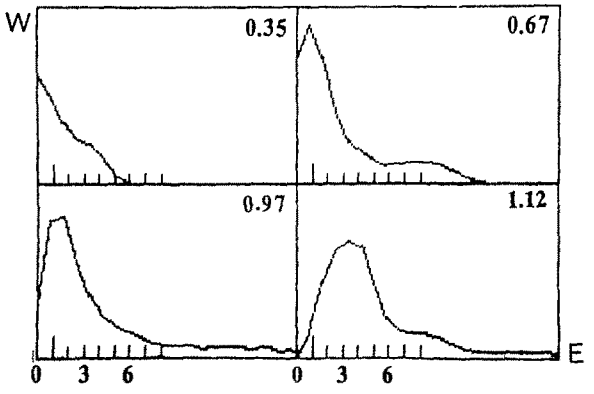

Fig. 5. Photoelectron spectra for half period $T/2=7.5$ and various field strengths. All other parameters are the same as in Figs. 3, 4

away from the potential center and the chance of recombination gets smaller. The only exception from this general rule is the case of classical resonance. The resonance peak is clearly seen in Fig. 4 which shows the dependence of ionization probability on the wave period. The resonance can be connected with the eigenfrequency of the unperturbed system $T_0=2\pi a/\sqrt{2U_0}$, but the dynamical shift is quite large.

The main result of our model calculations are photoelectron spectra. They can be obtained by counting the number of trajectories ending with a given energy. Four examples of such spectra are presented in Fig. 5. In this figure the field strength K varies from 0.35 to 1.12. On the energy axis we have plotted the positions of the individual photon peaks which should be visible had we been using quantum theory. Observe, that the maximum of the spectrum becomes shifted towards higher energies with the increasing field strength. Also the values of the spectra tend to zero at zero photoelectron energy.

In the classical model discussed in this paper we could not get peaks in the photoelectron spectrum corresponding to absorption of a prescribed number of photons. What we can do, however, is to compare the envelope of the spectrum obtained in our calculations with the observed envelope. Qualitative comparison seems very convincing – the classical model exhibit the main features of the photoelectron spectra, namely the dissapearance of the low energy peaks in an intense field and the general shape of the envelope.

We may now formulate a conjecture concerning the nature of the ATI spectrum observed in real systems. Peak inversion, which is the most intriguing feature of ATI, may be due to the dynamics of the ionization by strong fields. Our model calculation shows, that indeed the spectrum exhibits the main features observed in real experiments. Ponderomotive force effects or space charge effects may affect the final spectra, but the general shape of spectra originate from the dynamics of the atom-field interaction. Of course our analysis is a very approximate one. However the approximations do not affect the dynamics of the atom-field interaction, but rather the way of description. Thus our approach of the atom-field interaction is complementary to other approaches, where the description of the system is accurate (quantum mechanics is used throughout) but the dynamics is an approximated one.

It should be pointed out, that most of theories of ATI [3–6] are based in this or that way on the idea of essential states. It was pointed out [7] that such an approach can be valid for fields not stronger than some critical intensity, typically in the range of 10^{14} W/cm^2. No models of ATI for higher intensities were formulated. Our phase averaging method is well suited for the study of strong field ionization, even above the threshold mentioned above. In fact, the stronger the field the more accurate the phase averaging method becomes. That is because the stronger the perturbing field the better the classical approximation works. This improvement is due to two reasons. The first is that the initial, ground state of the atom becomes a nonstationary state in the external field. The stronger field the further from the stationary state the initial state becomes. Therefore we may look at the evolution of the initial state as a rapid flow of the wave function towards a new stationary configuration. The initial ground state in a strong field becomes in fact a highly excited one. The second reason is that the process of ionization in strong fields becomes very fast. In fact we have seen that it takes just a few optical periods for many electrons to get out of the potential well. If a process is that fast the quantum mechanical diffusion has no time to fully manifest itself. The motion of the wave packet is mostly determined by classical flow of the probability and

most of the quantum mechanical features have not enough time to develop.

We are grateful to M. Lewenstein, K. Rzazewski and J. Zakrzewski for fruitful discussions. The work was partially supported by Polish Ministry of Sciences, grand CPBP.01.07. and by Alexander von Humboldt Stiftung.

Appendix

In the Appendix we will derive the map corresponding to the equations of motion given by the hamiltonian (1). We have to solve separately equations of motion from time $t=nT/2^+$ (just after n-th impulse) to $t=(n+1)\,T/2^-$ (just before $n+1-$th impulse). During infinitely short impulse the position remains unchanged but the momentum changes: $p_{n+}=p_{n-}+(-1)^{n+1}K$. It is convenient to introduce new variables: $x'=\sinh(x)$ and $p'=p\cosh(x)$. We will discuss the cases of positive and negative energies separately. For the case of negative energy one obtaines the following equations of motion in the new variables:

$$\frac{dx'}{dt}=p',$$

$$\frac{dp'}{dt}=-\omega^2 x$$

with the standard solutions

$$x'(t)=B\sin(\omega t),$$

$$p'(t)=\omega B\cos(\omega t),$$

where $\omega=\sqrt{-E}$ and $B=\sqrt{(E+1)/(-E)}$. Thus for all the case of negative energies the map reads:

$$x_{n+1}=\operatorname{arsinh}[\sqrt{(E_n+1)/(-E_n)}\sin(\omega T/2+\phi_n)],$$

$$p_{n+1}=\sqrt{2(E_n+1)}\cos(\omega T/2+\phi_n)/\cosh(x_{n+1})+(-1)^n K,$$

where

$$E_n=p_n^2/2+U(x_n),$$

$$\phi_n=\arctan[\sqrt{-2E_n}\sinh(x_n)/p_n\cosh(x_n)].$$

By the same arguments we find that for negative energy the map reads:

$$x_{n+1}=[\operatorname{sign}(p_n)\sqrt{(E_n+1)/E_n}\sinh(\Omega T/2+\psi_n)],$$

$$p_{n+1}=\operatorname{sign}(p_n)\sqrt{2(E_n+1)}\cosh(\Omega T/2+\psi_n)/\cosh(x_{n+1})+(-1)^n K,$$

where $\psi_n=\operatorname{arsinh}[\operatorname{sign}(p_n)\sqrt{E_n/(E_n+1)}\sinh(x_n)]$ and $\Omega=\sqrt{2E_n}$.

For the case of zero energy the map is:

$$x_{n+1}=\operatorname{arsinh}[\sinh(x_n)+p_n\,T/2\cosh(x_n),$$

$$p_{n+1}=p_n\cosh(x_n)/\cosh(x_{n+1})+(-1)^n K.$$

Thus in order to perform numerical iterations of the classical map it is necessary to check the sign of the energy after each kick and then apply the appropriate transformation.

References

1. Agostini, P., Fabre, F., Mainfray, G., Petite, G., Rahman, N.: Phys. Rev. Lett. **42**, 1127 (1979); Kruit, P., Kimman, J., van der Wiel, M.: J. Phys. B**14**, L597; Fabre, F., Petite, G., Agostini, P., Clement, M.: J. Phys. B**15**, 1353 (1982); Lompre, L.A., l'Huiller, A., Minfray, G., Manus, C.: JOSA B**2**, 1906 (1985)
2. Muller, H., Tip, A., van der Wiel, M.: J. Phys. B**16**, L679 (1983); Mittleman, M.H.: Prog. Quantum Electr. **8**, 165 (1984); Chu, S.I., Cooper, J.: Phys. Rev. A**32**, 2769 (1985)
3. see Lompre, L.A. et al. [1]
4. Crance, M.: to be published
5. Yergeau, F., Petite, G., Agostini, P.: (to be published)
6. Bialynicka-Birula, Z.: J. Phys. B**17**, 3091 (1984); Edwards, M., Pan, L., Armstrong, L.: J. Phys. B**17**, L515 (1984); J. Phys. B**18**, (1985): Deng, Z., Eberly, J.H.: Phys. Rev. Lett. **53**, 1810 (1984); JOSA B**2**, 486 (1985); Lewenstein, M., Mostowski, J., Trippenbach, M.: J. Phys. B**18**, L461 (1985); Grochmalicki, J., Kuklinski, J.R., Lewenstein, M.: J. Phys. B (to be published); Rzazewski, K., Grobe, R.: Phys. Rev. Lett. **54**, 1729 (1985); Phys. Rev. A**33**, 1855 (1986); Dulcic, A., Eberly, J.H.: (to be published); Becker, W., Schlicher, R.R., Scully, M.O.: J. Phys. B**19**, L785 (1986)
7. Mostowski, J., Rzazewski, K.: (to be published)
8. Jones, D.A., Leopold, J.G., Percival, I.C.: J. Phys. B**13**, 31 (1980); Jensen, R.: Phys. Rev. A**30**, 36 (1984); Leopold, J.G., Richards, D.: J. Phys. B**18**, 3369 (1985); van Leeuven, K.A., et al.: Phys. Rev. Lett. **55**, 2231 (1985)
9. Mayer, I.L., Miranda, L., Tang, B.Y., Galvao, R.M.: J. Phys. B**18**, 3835 (1985)
10. Blümel, R., Meier, R.: Preprint Rehovot, WIS/84-132 (to be published)
11. Greene, J.M.: J. Math. Phys. **20**, 1183 (1979); Chirikov, B.V.: Phys. Rep. **52**, 263 (1979); Zaslavsky, G.M.: Phys. Rep. **80**, 157 (1981); Casati, G., Guanieri, I.: Commun. Math. Phys. **95**, 121 (1984); Shepelyanski, D.L.: Physica **8**D, 208 (1983)
12. Rzazewski, K., Mostowski, J.: Phys. Rev. A: (to be published)

J. Mostowski
Max-Planck Institut für Quantenoptik
D-8046 Garching
Federal Republic of Germany

K. Zyczkowski
Institute of Physics
Jagiellonian University
Reymonta 4
PL-30-059 Cracow
Poland